## Dalton Transactions



#### COMMUNICATION

View Article Online



**Cite this:** *Dalton Trans.*, 2021, **50**, 480

Received 2nd November 2020, Accepted 1st December 2020 DOI: 10.1039/d0dt03775c

rsc.li/dalton

# Snapshots of "crystalline" salt-water solutions of inositol hexaphosphate conformers†

Sandeep Kaur, Subhamay Pramanik, Victor W. Day and Kristin Bowman-James \*\*

Supramolecular insight to intra- and inter-ionic interactions in two inositol hexaphosphate conformers as a function of pH was enabled by NMR and crystallographic studies. These findings also shed light on the complex interactive roles of extended salt-water arrays through the crystal "solution" lattice.

Given worldwide concern over dwindling supplies of readily accessible phosphorus, <sup>1,2</sup> inositol hexaphosphates (IP<sub>6</sub>s), present a potential globally-available organic source of phosphorus. These biomolecules are not only among the most prevalent organophosphates in soils, but are also an important source of concentrated phosphorus throughout the plant kingdom.<sup>3,4</sup> Neutral phytic acid (the *myo*-stereoisomer) and its anions contain almost 30% by weight phosphorus. For many years interest in these phosphorus pools, especially among agricultural chemists and biologists, has been generated by their widespread presence and multiple functions in the plant world.<sup>5</sup>

With this communication we report the first two crystal structures of a scyllo-IP<sub>6</sub> metal ion salt. These structures also represent the first structures of both the high and low pH conformers of any stereoisomer of IP<sub>6</sub> with the same metal ion. scyllo-Inositol-1,2,3,4,5,6-hexakis-phosphate, scyllo-IP<sub>6</sub>, is the second most prevalent stereoisomer of the IP<sub>6</sub>s. The most commonly occurring IP<sub>6</sub> is the myo-stereoisomer, known as phytate. These structures also represent the fourth and fifth crystallographic reports of any IP<sub>6</sub> salt. The first structure, sodium [Na]<sub>12</sub>[IP<sub>6</sub>], was published long ago in the early 1970s. After over 50 years the second and third salts,  $[Zn]_{10}[H_2IP_6]_2$  and  $[K]_3[H_9IP_6]^9$  were reported, in 2017 and 2019, respectively. To date, solution and modeling investi-

Department of Chemistry, University of Kansas, 1567 Irving Hill Road, Lawrence, Kansas 66045, USA. E-mail: kbjames@ku.edu

gations have enabled excellent predictions as to hydrogen atom positions and metal ion binding sites at various pHs. 10 Clearly, however, crystal structures are needed to fill in the missing gaps since they provide exact pictures of intra- and inter-molecular interactions, including metal ion binding sites.

Additionally, given the large numbers of water molecules found in these crystals, the two structures provide a rare opportunity to view what we believe could be a crystalline model of what happens in aqueous salt-water solutions. Ion pair interactions have intrigued scientists for years, and it is now well-established that salt solutions do not normally show ideal behavior as a result of the multiple possibilities for ionic interactions. <sup>11,12</sup> These particular IP<sub>6</sub> salts are more complex than simple M<sup>+</sup>X<sup>-</sup> salts, however, since they are salt-water solutions of larger highly-charged organic ions with multiple anionic sites that are counterbalanced by multiple monopositive metal ions. While this report will cover some of the crystallographic aspects of the salt-water structure, more in-depth structural ramifications of this solvent system will be discussed elsewhere.

At physiological pHs, IP6s are multiply deprotonated where charges are about -7 to -8 out of a total possible charge of -12.10,13,14 Given their large negative charges, even at mid-pH ranges, IP6s behave as metal ion sponges, frequently forming highly insoluble salts. This chemistry has led to the classification of the most prevalent of the IP<sub>6</sub> stereoisomers, phytate (myo-inositol-1,2,3,4,5,6-hexakisphosphate), as an anti-nutrient.13 Phytate has major roles in vivo in the plant kingdom that include signal transduction, cell regulation, storage and retrieval of phosphorus, as well as numerous other functions, some of which have yet to be identified. 5,13,15 It has eight other possible stereoiosomers, although not all have been observed in Nature.4 The scyllo isomer has been reported as varying from 20 to 50% of the total IP6 in different soils. Although scyllo-IP6, is the second most prevalent of the IP6 stereoisomers, few studies of pure scyllo-IP6 have been reported. Also, not much is known about its function, if any. It has been

<sup>†</sup>Electronic supplementary information (ESI) available: For materials, instrumentation, synthetic procedures, spectroscopic analysis and X-ray crystallographic studies. CCDC 2027581 and 2027582. For ESI and crystallographic data in CIF or other electronic format see DOI: 10.1039/d0dt03775c

Dalton Transactions Communication

Scheme 1 Conformation flip from low to high pH of scyllo-IP<sub>6</sub><sup>n-</sup>.

suggested, however, to be a product of degradation of phytate by epimerization (Scheme 1).<sup>4</sup>

At low pHs the phosphates of the *scyllo* and *myo* stereo-isomers are predominantly at less hindered equatorial (e) rather than axial (a) positions. At higher pHs, they undergo conversions to mostly axial phosphates, *i.e.*, from 1a5e to 5a1e for the *myo*- and 6e to 6a for the *scyllo*-IP<sub>6</sub>. These changes, generally between pH 9 and 10, have been extensively studied both experimentally (mainly by NMR) and computationally, but are primarily limited to the more prevalent *myo*-IP<sub>6</sub>. The pH at which the conformation change occurs depends on a number of factors, including metal counterion size and charge. Much chemistry still needs to be explored in order to even begin to understand the complex chemistry of these highly phosphorylated biomolecules.

Our interest in the *scyllo*-IP<sub>6</sub> stereoisomer stems from our earlier studies of the dipotassium salt of *myo*-IP<sub>6</sub>, where NMR revealed small amounts of impurities, including inorganic phosphate (PO<sub>4</sub><sup>3-</sup>) and other possible isomers of inositol. One of these we subsequently identified as the *scyllo* stereoisomer, which was present as approximately 3% of the phytate sample. We were later able to isolate crystals of a *scyllo* macrocyclic complex. Here we report the crystal structures of the 6a and 6e conformers of the sodium salts of *scyllo*-IP<sub>6</sub><sup>8-</sup> and *scyllo*-IP<sub>6</sub><sup>12-</sup>, respectively, salts potentially found in Nature.

Crystals of the 6a conformer suitable for X-ray were obtained at pH 12.68 from an aqueous solution by vapor diffusion of acetone. The asymmetric unit contains 1.5 scyllo- $IP_6^{12-}$  ions, 18 Na<sup>+</sup> ions, and 60.8 molecules of water:  $\{[Na]_{12}[C_6H_6(PO_4)_6]\}_{1.5}\cdot 60\cdot 8H_2O$ . Crystals of the 6e conformer were isolated from vapor diffusion of acetone into an aqueous solution of the Na<sup>+</sup> salt at pH 6.36. This conformer,  $[Na]_8[C_6H_6(HPO_4)_4(PO_4)_2]\cdot 26H_2O$ , has four singly-charged  $-P(=O)(OH)(O^-)$  (P1, P1' and P2, P2') and two doubly charged  $-P(=O)(O^2^-)_2$  (P3, P3') phosphates. Clearly, for both salts the large volume of water molecules of crystallization plays a major role in the crystal structure. Given the fact that the salts are surrounded by "salt" water solutions, these structures also potentially shed light on water interactions that could be mirrored in the solution structures as well.

In the high pH 6a conformer, there are two crystallographically independent *scyllo* ions, one without any internal symmetry, P1–P6 (*scyllo-1*) and one with an inversion center, P7–P9 and P7′–P9′ (*scyllo-2*). The interionic associations with the

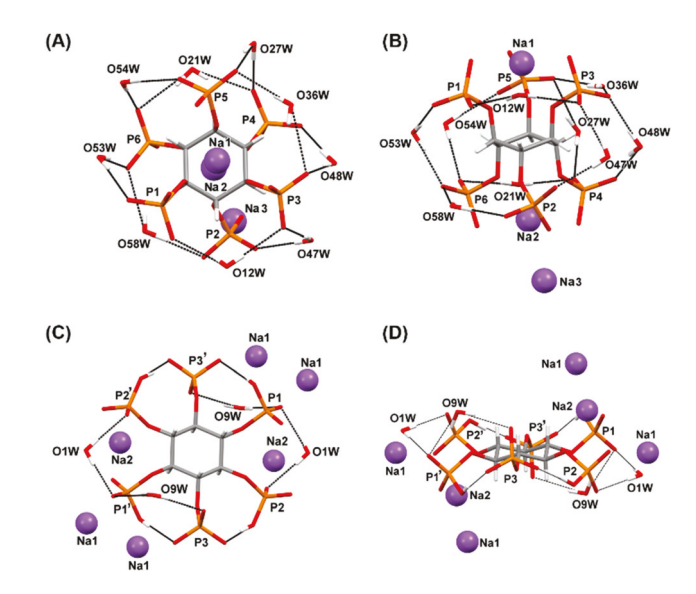


Fig. 1 Overhead and side perspective views of chelated water molecules for the 6a conformation for *scyllo-1*, (A) and (B), respectively; and corollary pictures of the 6e conformations, (C) and (D), respectively, showing Na<sup>+</sup> ions within 3.0 Å of the center of the inositol.

adjacent Na<sup>+</sup> ions and phosphate chelating network to surrounding water molecules for the two *scyllo* ions are almost identical (Fig. 1(A) and (B) and Fig. S1(A) and (B)†). In addition to the three Na<sup>+</sup> ions, the immediate coordination sphere around *scyllo-1* consists of nine chelated water molecules. There are five water bridges between the upper and lower phosphates (P1 with P6; P3 with P2 and P4; P5 with P4 and P6) and two around the upper phosphates and two around the lower phosphates (P6 with P2 and P4; P3 with P5 and P1) with hydrogen bonding distances ranging from of 2.695(3) to 3.034(5) Å. The water network in *scyllo-2* is similar, but with six waters bridging upper and lower phosphates and one chelating between upper and one between lower phosphates (Fig. S1(A) and (B)†).

The strong chelation of each set of upper and lower phosphates to a single Na<sup>+</sup> ion immediately stands out in both scyllo-1 and -2 anions. Multiple interactions of these Na<sup>+</sup> ions with all three phosphates are the most obvious structural characteristic of the high pH 6a conformer. Similar chelation was observed with two axial phosphates for the high pH 5a1e conformer of the sodium salt of phytate. 6,7 The chelation of all three phosphates to a single Na+ ion in scyllo-IP6 certainly serves to offset intramolecular repulsions arising from the dinegative charges on each of the phosphates. The axial Na<sup>+</sup> ions are held to each of the three surrounding phosphate groups by interactions with one of the terminal oxygen atoms and a second with the ester oxygen atom, with distances ranging from 2.410(2) to 2.624(2) (Å). The coordination spheres of the scyllo Na1 and Na2 ions are completed by axial water molecules, as seen for the two water-joined scyllo-1s (Na1 and Na2, Fig. 2(A)) and in the single scyllo-2 (Na15 and Na15', Fig. S1(C)†), leading to "capped trigonal prism" seven(A) Na3 P2 P3 Na1 P4 P6 P5 Na1 P2 P3 Na1 P2 P3 Na1 P2 P3 Na1 P3 N

Communication

Fig. 2 Perspective views of translationally-related dimer pairs of (A) 6a and (B) 6e conformation.

coordinate geometries. An additional Na $^+$  ion (Na3) in *scyllo-1* interacts directly with one of the terminal P2 oxygens, Na $^+$ -O $^-$  = 2.299(2) Å. However, interestingly, in *scyllo-2* there are no nearby Na $^+$  ions. The presence of an additional Na $^+$  ion in *scyllo-1* is one of the few major differences between the two independent anions.

In the 6e conformer, *scyllo*-IP<sub>6</sub><sup>8-</sup>, with a lower concentration of Na<sup>+</sup> ions, phosphate intra- and inter-molecular interactions are somewhat different. The four hydrogens on the six phosphates provide for intramolecular hydrogen bonding unlike in the *scyllo*-IP<sub>6</sub><sup>12-</sup>. The immediate coordination sphere of the 6e conformer consists of six Na<sup>+</sup> ions and four chelated water molecules. Singly protonated phosphates, P1 and P2 and their symmetry equivalents are both hydrogen bonded to P3 directly through P-OH····O-P interactions, while phosphate oxygens from P1/1' and P2/2's form chelate bridges to each other through intervening O1W/1'W water molecules, and P1/1' and P3/3' phosphates through adjacent O9W/9'W waters (Fig. 1(C) and (D)).

Adjacent Na<sup>+</sup> ions interact only with the monoprotonated phosphates (the two P 1s and P 2s). Two inversion related Na2 ions bridge symmetry-related P1–O<sup>-</sup>...Na2<sup>+</sup>...O=P2 and four symmetry-related Na 1s are bound to two Na1...O=P 1s and two Na1...HO-P 1s (Fig. 1(C) and (D)) (Fig. 2(B)). The dinegatively charged P3/3' phosphates have no direct interactions with sodium ions, but two are interlocked *via* hydrogen bonds with neighboring P1/1's and P2/2's (Fig. 1(C)).

The water networks surrounding the two conformers are extensive. Hydrogen atoms on all 26 (6e conformer) or almost all 60.8 (6a conformer) of the water molecules were located by difference maps and were initially refined isotropically (see ESI†). There are significant concentrations of Na<sup>+</sup> ions in both water networks, leading to "salt-water" molecular lattice arrays,  $Na_x(H_2O)_y^{x+}$ . These include salt-water buffer zones around each *scyllo* ion (Fig. S2 and S3†).

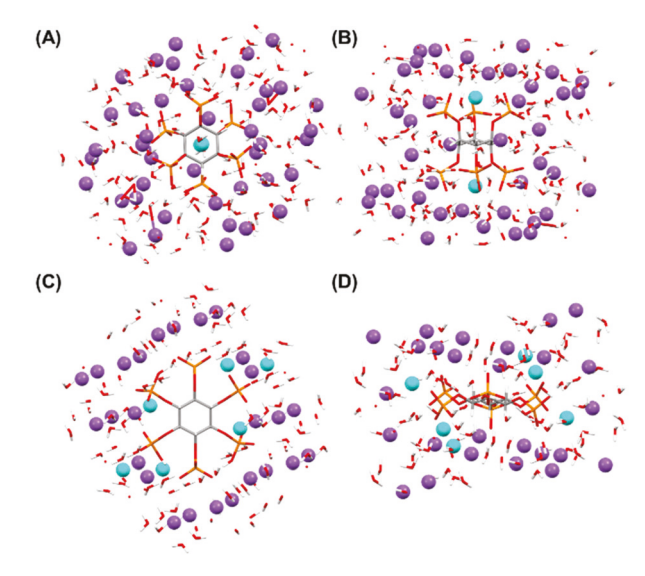


Fig. 3 Overhead and side views, respectively, of salt-water buffer zones around single *scyllo* ions showing: (A) and (B) 6a conformations (*scyllo-2*); (C) and (D) 6e conformations. Sodium ions are represented by balls and waters and *scyllo-IP* $_6$  by sticks. Turquoise balls represent Na $^+$  ions directly interacting with the *scyllo* phosphates.

The salt-water buffer layer only begins to describe the extensive salt-water network throughout the crystal lattice for both conformers (Fig. 3 and Fig. S4†). Both the 6a and 6e conformers have numerous salt-water layers that bridge between and among surrounding *scyllo*-IP<sub>6</sub>s and result in a highly interconnected array of *scyllo* groups within a salt-water sea. While not in direct contact with the *scyllo*-IP<sub>6</sub> ions, Na3 and Na4 of the 6e conformation are, instead, major contributors to seemingly independent salt-water-like chains through the channels separating the anions (Fig. 4).

Solution NMR spectra of the scyllo-IP6 ion are much simpler than those of phytate due to the high symmetries of the 6a and 6e conformations. Most of the previous NMR studies of phytate are <sup>31</sup>P as opposed to <sup>1</sup>H NMR, due to the complexity of the proton chemistry in solution. Yet since the myo-stereoisomer (phytate) is by far the most prevalent of the IP6s, these have been studied much more extensively, including an in-depth comparison of the NMRs along with theoretical studies of selected metal ion salts. 12 A recent review by Kremer, Bianchi and co-workers, nicely summarizes previous studies of phytate, especially including more recent supramolecular host-guest reports. 13 In our recent report of the crystal structure of the potassium salt of phytate, [K]<sub>3</sub>[myo-IP<sub>6</sub>], we focussed on the <sup>1</sup>H NMR as a function of pH. <sup>9</sup> However, to our knowledge, this is the first comparison of the <sup>1</sup>H (and <sup>31</sup>P) NMRs of pure alkali metal myo- and scyllo-stereoisomers of any of the inositol hexaphosphates.

The NMR trends of the sodium salt of *scyllo*-IP<sub>6</sub> are very similar to those observed for phytate except for their simplicity, which makes it easier to observe the conformation change from 6e to 6a. The *scyllo* NMRs were obtained in a range from pH 6.36 up to 12.84. The pH of the purchased sodium salt for

**Dalton Transactions** 

Fig. 4 Views of salt-water channels containing Na4 and Na5 (space-filled views) for  $scyllo-IP_6$  in the 6e conformation.

the *scyllo*-IP<sub>6</sub> was chosen as the initial pH for both  $^{1}$ H and  $^{31}$ P spectra since it would require no added acid for the baseline measurement. The  $^{1}$ H spectra consist of a broadened doublet throughout, as a result of  $^{1}$ H- $^{31}$ P coupling with the phosphate associated with the same carbon atom,  $J_{\rm HP}$  = 5.6 Hz.

Starting at pH 6.36 (4.24 ppm) for the <sup>1</sup>H spectra, the pH titration of scyllo-IP6 showed slight upfield shifts (Fig. 5A and Table S1†). By pH 8.06 (4.18 ppm) the signal started to broaden. At higher pHs the signal was almost imperceptible and shifted downfield to 4.42 ppm. A doublet emerged at pH 10.06, at which point the maximum downfield shift had been achieved, and the conversion from 6e to 6a was essentially complete. The broad signals between pH 8 and 10 are most probably due to rapid equilibria between the two conformers on the NMR timescale. At higher pHs, the signals remained relatively unchanged at 4.53 ppm with increasing basicity. The <sup>31</sup>P chemical shifts are likewise very simple, consisting of a singlet, which makes its way downfield with increasing pH (Fig. S5A and Table S2†). The ESI-MS (+ve ion mode) spectra provide additional evidence for the -8 and -12 charges on the crystals (Fig. S6†).

The <sup>1</sup>H NMR spectra of the *myo* salt are quite similar to those of the *scyllo*-IP<sub>6</sub> when following the *CH*5 protons, which we thus used in our comparisons (Fig. 5(B) and Table S1†). The <sup>1</sup>H chemical shifts follow a similar slight upfield then downfield pattern. By pH 10.06 the lower pH signals of the

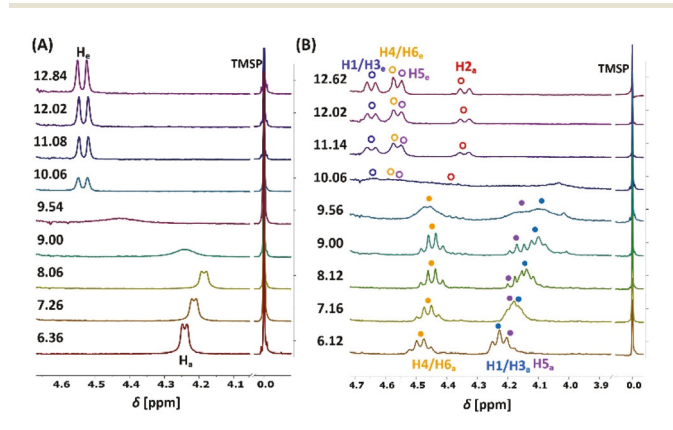


Fig. 5  $\,^{1}$ H NMR spectra (400 MHz) as a function of pH (Na(OH)) in D<sub>2</sub>O at 25  $\,^{\circ}$ C starting with the (A) the Na $^{+}$  salt of scyllo-IP<sub>6</sub> (10 mM) at pH 6.36, and (B) the Na $^{+}$  salt of myo-IP<sub>6</sub> (20 mM) at pH 6.12. Trimethylsilylpropanoic acid (TMSP) was used as an internal reference.

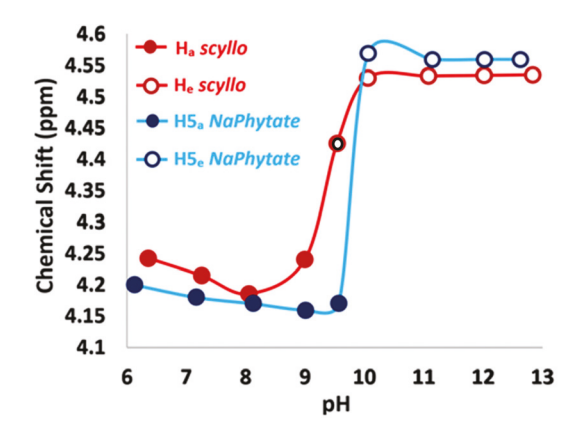


Fig. 6 Comparison of chemical shift changes for the *scyllo* CH signals and the myo CH<sub>5</sub> signals as a function of pH. Red circle with black lining refers to a fast equilibrium between both conformers.

*myo* salt have just about disappeared while shifting downfield, and only begin to sharpen again at pH 11.14. The use of the *CH*5 signal correlates very well with those of the *scyllo* stereo-isomer (Fig. 6 and Table S1†), down to similar ppms. Similar trends are observed for the <sup>31</sup>P NMRs for the *scyllo* and *myo* conformers (Fig. S5, and Table S2†).

In conclusion, the two conformers of the *scyllo*-IP<sub>6</sub> anions reveal different structural patterns, partly as a result of the lack and presence of P–OH groups for the 6a and 6e conformations, respectively. Both sodium ions and water play prominent roles in the two structures. Crystallographically most striking, however, are (1) the small number of direct Na<sup>+</sup> contacts with the IP<sub>6</sub> anions (three for *scyllo-1* and two for *scyllo-2* for the 6a conformer and six for the 6e conformer), and (2) the extensive solvent layers and buffer zones surrounding both *scyllo*-IP<sub>6</sub> conformers. As a result of these crystallographic findings, the two structures provide snapshots of what is potentially occurring in solution. To our knowledge, observing such extensive salt-waters of crystallization is unusual in small molecule structures.

#### Conflicts of interest

There are no conflicts to declare.

### Acknowledgements

The authors thank the National Science Foundation (CHE-1710535) for support of this work and (CHE-0923449) for the purchase of the X-ray diffractometer. The authors also thank Dr Justin T. Douglas, Director of the NMR Laboratory at the University of Kansas, for helpful NMR discussions.

#### Notes and references

Communication

- 1 NSF FEW Workshop Report on Closing the Human Phosphorus Cycle, Arlington, VA, June 8-9, 2015.
- 2 J. J. Elser and E. Bennett, Phosphorus: A Broken Biogeochemical Cycle, Nature, 2011, 478, 29-31.
- 3 B. L. Turner, M. J. Papházy, P. M. Haygarth and I. D. McKelvie, Inositol Phosphates in the Environment, Philos. Trans. R. Soc., B, 2002, 357, 449-469.
- 4 M. P. Thomas, S. J. Mills and B. V. L. Potter, The "other" inositols and their phosphates: synthesis, biology, and medicine (with recent advances in myo-inositol chemistry), Angew. Chem., Int. Ed., 2016, 55, 1614-1650.
- 5 V. myo-Inositol-1,2,3,4,5,6-hexakisphosphate, Phytochemistry, 2003, 64, 1033-1043.
- 6 G. E. Blank, J. Pletcher and M. Sax, Biochem. Biophys. Res. Commun., 1971, 44, 319-325.
- 7 G. E. Blank, J. Pletcher and M. Sax, Acta Crystallogr., Sect. B: Struct. Crystallogr. Cryst. Chem., 1975, 31, 2584-2592.

- 8 K. Cai, F. Sun, X. Liang, C. Liu, N. Zhao, X. Zou and G. Zhu, J. Mater. Chem. A, 2017, 5, 12943-12950.
- 9 M. Reinmuth, S. Pramanik, J. T. Douglas, V. W. Day and K. Bowman-James, Eur. J. Inorg. Chem., 2019, 2019, 1870-1874.
- 10 N. Veiga, J. Torres, I. Macho, K. Gómez, G. González and C. Kremer, Dalton Trans., 2014, 43, 16238-16251.
- 11 B. Gibb, Nat. Chem., 2018, 10, 797-798.
- 12 N. F. A. van Vegt, K. Haldrup, S. Roke, J. Zheng, M. Lund and H. J. Bakker, Chem. Rev., 2016, 116, 7626-7641.
- 13 C. Kremer, J. Torres, A. Bianchi, M. Savastano and C. Bazzicalupi, Coord. Chem. Rev., 2020, 419, 213403-213421.
- 14 N. Veiga, J. Torres, S. Domínguez, A. Mederos, R. F. Irvine, A. Diaz and C. Kremer, J. Inorg. Biochem., 2006, 100, 1800-1810.
- 15 V. Raboy, Plant Sci., 2009, 177, 281-296.
- 16 S. Pramanik, V. W. Day and K. Bowman-James, Chem. Commun., 2020, 56, 3269-3272.